Lagrangian Coherent Structures in the Elliptic Restricted Three-body Problem and Space Mission Design

IEPC-2013-414

Presented at the 33^{rd} International Electric Propulsion Conference, The George Washington University, Washington, D.C., USA October 6–10, 2013

Lorenzo Provinciali* and Michele Mastropietro†
Università di Pisa, Pisa, 56100, Italy

Pierpaolo Pergola‡ and Mariano Andrenucci§
Alta S.p.A., Pisa, 56100, Italy

Interplanetary transfers in multi-body gravitational regimes can take high advantage from the exploitation of invariant manifolds dynamics, ballistic structures separating transfer from non-transfer trajectories. This allows a spacecraft placed inside a well chosen invariant manifold to reach the target destination following the natural dynamics of the system, without any propulsive needs. Invariant manifolds, however, can only be computed in autonomous dynamical systems, like the Circular Restricted Three-body Problem. Any generalization of such a model leads to non-autonomous systems where Lagrangian Coherent Structures can be used as the natural manifold generalization. The Elliptic Restricted Three-body Problem, for instance, takes into account the eccentricity of the attractive body orbits and its chaotic behavior can only be studied by means of such a tool. The aim of the paper is to use the Lagrangian Coherent Structures in the Elliptic Restricted Three-body Problem to allow for the usage of this more refined model since the early mission design phases. A methodology to exploit this tool for interplanetary transfers in the Solar System is presented together with some applications for an Earth-Jupiter transfer. The idea is to consider a three-phase transfer, a single-burn Earth escape phase, an interplanetary coasting phase within a specific Lagrangian Coherent Structure of the Earth-Jupiter system, and a final bi-impulsive capture phase within the Jupiter sphere of influence. It is shown that all the transfers can be designed by means of a single Finite Time Lyapunov Exponents map and the procedure outlined is able to identify all transfer trajectories sought. In addition also the lowest Δv or shortest transfer time paths can be identified by means of a grid search approach. The methodology is first used for designing a specific transfer mission and in a second phase for carrying out a parametric study on all possible transfer dynamics and departure conditions.

*Master Student, Università di Pisa, Italy, lorenzo.provinciali@gmail.com.
†Master Student, Università di Pisa, Italy, michele.mastropietro@gmail.com.
‡Project Manager, Alta, Pisa; Ph.D.;p.pergola@alta-space.com.
§President, Alta, Pisa; Professor, Department of Aerospace Engineering., Università di Pisa, Italy; m.andrenucci@alta-space.com.

Nomenclature

μ	= mass parameter
e	= orbit eccentricity
a	= orbit semi-major axis
f	= true anomaly
v_∞	= hyperbolic excess velocity
$\dot{x}$	= x component of the spacecraft velocity in the synodic frame
$\dot{y}$	= y component of the spacecraft velocity in the synodic frame
$\dot{x}_E$	= x component of the Earth velocity in the synodic frame
$\dot{y}_E$	= y component of the Earth velocity in the synodic frame
$M_\oplus$	= Earth mass
a_h	= semi-major axis of escape hyperbola
$R_\oplus$	= Earth mean radius
h	= height of LEO parking orbit from Earth surface
$\boldsymbol{h}$	= orbit angular momentum
v_p	= velocity at the perigee of the escape hyperbola
R_{SOI}	= radius of the sphere of influence
r_p	= pericenter radius of the target orbit
r_a	= apocenter radius of the target orbit
M_t	= target planet mass
(v_{x_t}, v_{y_t})	= target planet orbital velocity in the heliocentric inertial reference frame
Δv_p	= velocity change at periapsis of target orbit
Δv_a	= velocity change at apoapsis of target orbit
Δv	= total velocity change
σ	= Finite Time Lyapunov Exponent field
ϕ	= dynamical system flow map

I. Introduction

New orientations in space mission design have seen the theory of dynamical systems playing a more and more important role. The trend of recent works,[1,2] is to make extensive usage of non-linear dynamical systems theory to gain insight into the chaotic behavior of multi-body models. The fundamental model used to study space mission beyond the classical Keplerian model is the Restricted Three-body Model. Such a model is a chaotic non-integrable model presenting a single first integral, equilibrium points, periodic orbits and ballistic solutions to/from these (invariant manifolds). It has been recognized that the study of invariant manifolds is a fundamental tool to identify several dynamics which can help to "organize" the chaos in the Circular Restricted Three-body Problem.[1]

Manifolds can be numerically computed and they have been widely used to take advantage of the natural dynamics of the system in space mission design. Previous works[1,2] dealt with the problem of interplanetary transfers in multi-body regimes even with low-thrust propulsion, heavily exploiting the invariant manifold approach.

Invariant manifolds, however, exist only in autonomous systems, and each generalization of the restricted three-body problem to more accurate models (e.g. taking into account additional gravity fields or the planet eccentricity) makes the resulting equations of motion non-autonomous.

Another useful and relatively new approach in the study of non-linear dynamical systems are Lagrangian Coherent Structures (LCS).[3] LCS are a generalization of the invariant manifolds concept to non-autonomous systems acting as a time dependent separatrices of different regions of motion. They originate from ideas commonly employed in the study of fluid flows. In fact, seeking for coherent dynamics and transport processes in flows is an ability that could significantly advance the capability to both understand and exploit fluid flows in engineering and natural systems. Peacock and Dabiri,[3] indicate that Leonardo Da Vinci was the first to study and capture fluid structures in water flowing through obstacles.[4]

LCS have been already used as a tool to study coherent structures regulating the motion of turbulent flows. The term was introduced by Haller[5] and Haller and Yuan,[6] who presented mathematical criteria for the existence of finite time attracting and repelling material surfaces. These surfaces can delineate regions of fluid for which the long-term evolution is qualitatively different, being a valid alternative to invariant manifolds. Applications of LCS can be found in several fields: from weather forecasting to transport in the ocean, from flapping wings flows to blood circulation and airway transport.[3,7]

LCS, in contrast with invariant manifolds, can be computed regardless of the type of the dynamical system.

The first possible generalization of the circular three body system is the Elliptic Restricted Three-body Problem. This model takes into account the eccentricity of orbits of the main attractors and consequently introduces the time (or equivalently the true anomaly of the smaller primary) in the equations of motion as an explicit variable. Gawlik[8] used the Sun-Mercury Elliptic Three-body System to show that BepiColombo spacecraft will follow an LCS in its journey towards Mercury. This is, however, one of the few examples of applications of such a tool to space mission design. The aim of the paper is to present a methodology for the exploitation of LCS applications in space mission design.

In particular in this paper (Sec. V) we introduce a methodology to design interplanetary transfers from Earth to other planets of the Solar System by exploiting Lagrangian Coherent Structures. These are computed considering a Planar Elliptic Three-body System whose primaries are the Sun and the target planet. An overview of the Elliptic Restricted Three-body Problem is presented in Sec. II, while Section III provides a brief summary of the concept of Lagrangian Coherent Structures and their computation techniques. Section IV shows the main features of the software developed to compute and visualize LCS in a Planar Elliptic Restricted Three-body System together with a couple of tests. After showing the mission design methodology in Sec. V, we provide an example considering a complete Earth-Jupiter transfer. Finally, a slightly modified methodology allowing more flexibility in the choice of mission design parameters is introduced in Sec. VII.

II. The Elliptic Restricted Three-body problem

The Circular Restricted Three-body Problem (CR3BP) studies the motion of a moving particle under the gravitational influence of other two massive bodies (primaries) assumed to revolve in circular orbits around their common center of mass. The Elliptic Restricted Three-body Problem (ER3BP) is the natural generalization of the CR3BP where the eccentricity of the primaries orbits is taken into account.

With the Elliptic Restricted Three-body Model it is possible to describe the long-time behavior of important dynamical systems in celestial mechanics, like asteroids and comets motion under the influence of the main solar system bodies or the evolution of the solar system itself. In fact, significant effects in the dynamics might be expected because of the eccentricity of the primaries orbits and, unlike the circular restricted three-body model, the elliptic model is able to take it into account.[9]

Similarly to the circular problem, the equations of motion of this system can be written in a compact form by considering a synodic non-dimensional reference system (see Fig. 1).

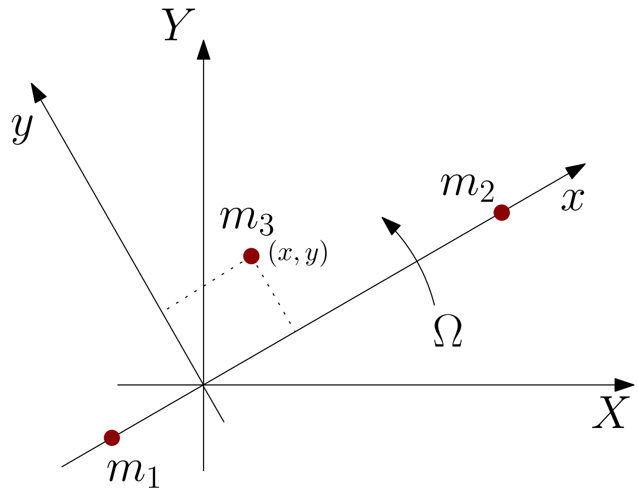

Figure 1. (X, Y) is the inertial reference frame, (x, y) is the synodic one which rotates with the angular velocity Ω of the two primaries (m_1 and m_2).

Non-dimensional distances are obtained by dividing dimensional length by the instantaneous distance ρ between the two attractive bodies. This distance is regulated by the formula:[10]

$$\rho = \frac{a(1-e^2)}{1+e\cos f} \tag{1}$$

where a and e are respectively the semi-major axis and the eccentricity of the system composed by the two primaries. The mass is normalized with respect to the total mass of the two primaries:

$$\mu_{1,2} = \frac{m_{1,2}}{m_1+m_2} \tag{2}$$

Following the definition, it is clear that $\mu_1 + \mu_2 = 1$. Assuming, without loss of generality, $m_1 > m_2$ it's possible to define the *mass parameter* $\mu = \mu_2$. It is defined in the interval $\mu \in [0, 1/2]$ so as

$$\mu_1 = 1-\mu; \qquad \mu_2 = \mu \tag{3}$$

Time is normalized by the quantity $\sqrt{\rho^3/(G(m_1+m_2))}$, where $G = 6.67\times10^{-11}$ m^3 kg^{-1} s^{-2} is the universal gravitational constant. In this way the rotation period of the two primaries around their common center of mass is 2π.

With this approach the ER3BP reference frame becomes pulsating as a function of the independent parameter, i.e. the true anomaly of the smaller primary, f. One major advantage of the synodic system is that the two primaries positions are fixed in time. They are $(-\mu,\ 0,\ 0)$ for m_1 and $(1-\mu,\ 0,\ 0)$ for m_2.

Equations of motion in the synodic frame can be obtained by the partial derivatives of a pseudo-potential function defined by:[10]

$$\omega(x, y, z, f) = \frac{1}{1+e\cos f}\left[\frac{1}{2}(x^2+y^2) + \frac{1-\mu}{r_1} + \frac{\mu}{r_2} + \frac{1}{2}\mu(1-\mu)\right] \tag{4}$$

where

$$r_1 = \sqrt{(x-x_1)^2+(y-y_1)^2+z^2} \tag{5}$$
$$r_2 = \sqrt{(x-x_2)^2+(y-y_2)^2+z^2} \tag{6}$$

Indicating with a dot the derivatives w.r.t. the independent variable f, the equations of motion are:

$$\begin{cases} \ddot{x} - 2\dot{y} = \dfrac{\partial \omega}{\partial x} \\ \ddot{y} + 2\dot{y} = \dfrac{\partial \omega}{\partial y} \\ \ddot{z} = \dfrac{\partial \omega}{\partial z} \end{cases} \tag{7}$$

To simplify the model, in the following we consider only the planar case neglecting the equation of z.

Another useful parameter is the energy of the system defined as:[1,8,9]

$$E(x, y, z, \dot{x}, \dot{y}, \dot{z}) = \frac{1}{2}\left(\dot{x}^2 + \dot{y}^2\right) + \omega(x, y, z, f) \tag{8}$$

This is the sum of the kinetic energy of a particle in the rotating non-dimensional reference frame and the pseudo-potential defined in Eq. (4). Such energy is the only first integral of the motion in the CR3BP ($e = 0$), whereas it is a time dependent (non conservative) function in the ER3BP.

III. Lagrangian Coherent Structures, a generalization of invariant manifolds

Invariant manifolds can only be computed in autonomous dynamical systems like the Circular Restricted Three-body Problem (CR3BP).[1] As soon as time plays a role in the mathematical model, Lagrangian Coherent Structures (LCS) are the generalization of manifolds.[11]

A generic dynamical system in a n-dimensional phase space ($\boldsymbol{x} \in \mathbb{R}^n$) can be defined via the differential equations:

$$\begin{cases} \dot{\boldsymbol{x}}(t) = \boldsymbol{v}(\boldsymbol{x}, t) \\ \boldsymbol{x}(t_0) = \boldsymbol{x}_0 \end{cases} \tag{9}$$

where $\boldsymbol{v}$ represents the set of ordinary differential equations of the first order regulating the motion of a test particle. A solution of this set of differential equations is the flow map $\phi(t_0, t; \boldsymbol{x_0})$, also expressed as $\phi_{t_0}^{t}(\boldsymbol{x_0})$, which represents the state of the system evolved to a final time t from an initial state $\boldsymbol{x_0}$ specified at time t_0. In general, LCS can be identified as 1-codimensional subspaces of the phase space, that is, $n-1$ dimensional surfaces.[12] Fundamental LCS properties are that they represent effective transport barriers and they subdivide the phase space into areas with different dynamical behavior.[6] A particle with initial conditions taken inside the boundary of a LCS will evolve bounded by the same LCS, being unable to cross that surface. At the same time, two different particles initially taken inside the same LCS will show a qualitatively similar evolution.

These properties are characteristics also belonging to the invariant manifolds; indeed LCS in CR3BP exactly match the invariant manifolds.[8,11] When eccentricity is taken into account in the Elliptic Restricted Three-body Problem (ER3BP) time dependence is introduced and invariant manifolds no longer exist, but LCS still do.[8]

A. Computation of Lagrangian Coherent Structures

Given a generic dynamical system, LCS can be identified with the ridges of the Finite Time Lyapunov Exponents (FTLE) field relative to that dynamical system.[8,12] In turn, FTLE are a measure of adjacent trajectories deformation after a finite time interval. To calculate the FTLE at some point $\boldsymbol{x}_0$ we need to compute the right Cauchy-Green tensor:

$$C = (\nabla \phi_{t_0}^{t})^T (\nabla \phi_{t_0}^{t}) \tag{10}$$

where $\nabla \phi$ can be obtained via finite differencing on a grid of points taken in the phase space (see Fig. 2):

$$\nabla \phi_{t_0}^{t} = \begin{bmatrix} \frac{\Delta x_1(t)}{\Delta x_1(t_0)} & \cdots & \frac{\Delta x_1(t)}{\Delta x_n(t_0)} \\ \vdots & \ddots & \vdots \\ \frac{\Delta x_n(t)}{\Delta x_1(t_0)} & \cdots & \frac{\Delta x_n(t)}{\Delta x_n(t_0)} \end{bmatrix} \tag{11}$$

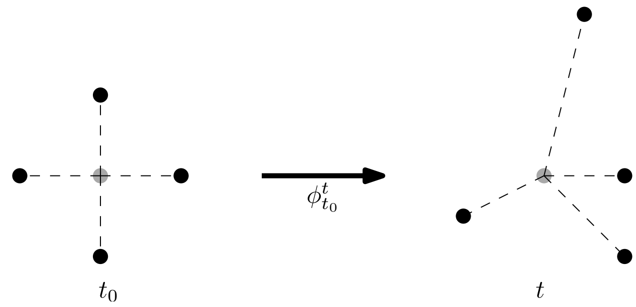

Figure 2. Deformation of adjacent initial points on a grid after the application of the flow map from t_0 to t.

FTLE (σ) for each point of the phase space is thus computed by means of the following equation,[5,8,12] fixing the integration time $t = T$:

$$\sigma(\boldsymbol{x}, t_0, T) = \frac{1}{|T|} \log \sqrt{\lambda_{\max}(C)} \tag{12}$$

where $\lambda_{\max}(C)$ is the largest eigenvalue of the tensor C (which by definition is positive defined).

Finally, to compute a LCS we need to extract the ridges from FTLE maps. As an example, Fig. 3 shows the FTLE ridge on a 2D grid; in general, however, ridges can be computed on higher dimensional phase space regions. More precisely a ridge is constituted by points, called *ridge points*, whose principal curvature is a local maximum.[12] To identify those points, image analysis tools can be used.[13]

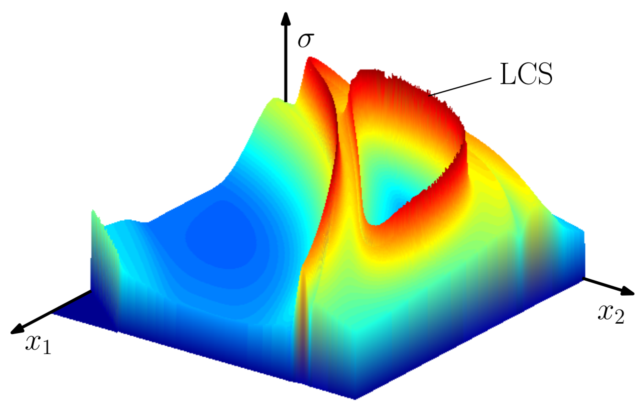

Figure 3. 3D view of FTLE map on a plane of the phase space. LCS can be identified as ridges of the FTLE map.

IV. LCS in the Elliptic Restricted Three-body problem

With the aim at exploiting LCS for mission analysis and design we implemented a tool to compute, extract and visualize the FTLE field both on 2D and 3D grids. As explained in Sec. III.A, a large number of integration of the equations of motion is required to compute LCS. The ER3BP, like the CR3BP, does not admit an analytical expression of the motion, thus, numerical integration procedures are required. To speedup the process the software has been written in a compiled language, C++, using the library Odeint[14] to perform the numerical integrations. Moreover, the code has been designed to be executed on multiple processors, as the task is highly parallelizable. The software is able to verify whether the trajectories will impact on the primaries, interrupting the integration accordingly. Finally, to visualize the results several Matlab routines implementing the visualization of 2D planes or 3D phase space regions were implemented together with tools for the detection of ridge points (post-processing phase). The following sections present two examples used to test the software.

A. Manifold computation in CR3BP using LCS

As LCS are actually the generalization of manifolds to non-autonomous cases, it is possible to cancel out the anomaly dependency in Eq. (4) by setting the eccentricity to zero in the ER3BP, thus making the equations of motion autonomous. In this way it is possible to model the (autonomous) circular case. Accordingly, in this case, the LCS should match the invariant manifolds sections as defined for the CR3BP.[11] Considering the Sun-Jupiter system ($\mu = 9.537 \times 10^{-4}$) with zero eccentricity, for instance, Fig. 4(b) can be obtained. In this case the grid has been done on the y coordinate and the associated velocity. The x coordinate has been fixed at $x = 1 - \mu$ and the other velocity coordinate, required to carry out the integration of Eq. (7), has been retrieved by fixing an energy value to $E = -1.519$ and using Eq. (8) with zero eccentricity. The energy value chosen is between those associated with the Lagrangian points L_2 and L_3 for the Sun-Jupiter system, a condition in which the motion in between the two primaries is allowed. Figure 4 shows the comparison with the same manifold computed by means of the classical approach.[1] The green area in Fig. 4(a) is the first intersection $\Gamma^{s,J}_{L_1,1}$ of the stable manifold of the circular Sun-Jupiter system starting from a Lyapunov orbit around L_1. It can be noted that it exactly matches with the area enclosed in the LCS (ridge of FTLE) computed.

This validates the tool for the zero eccentricity case, providing a more general tool for the computation of such a kind of structures. In addition, by changing the integration time (T in Eq. (12)), also the subsequent intersections with the LCS plane can be found and one numerical experiment showed that also these additional intersections match with the higher order intersections of manifolds.

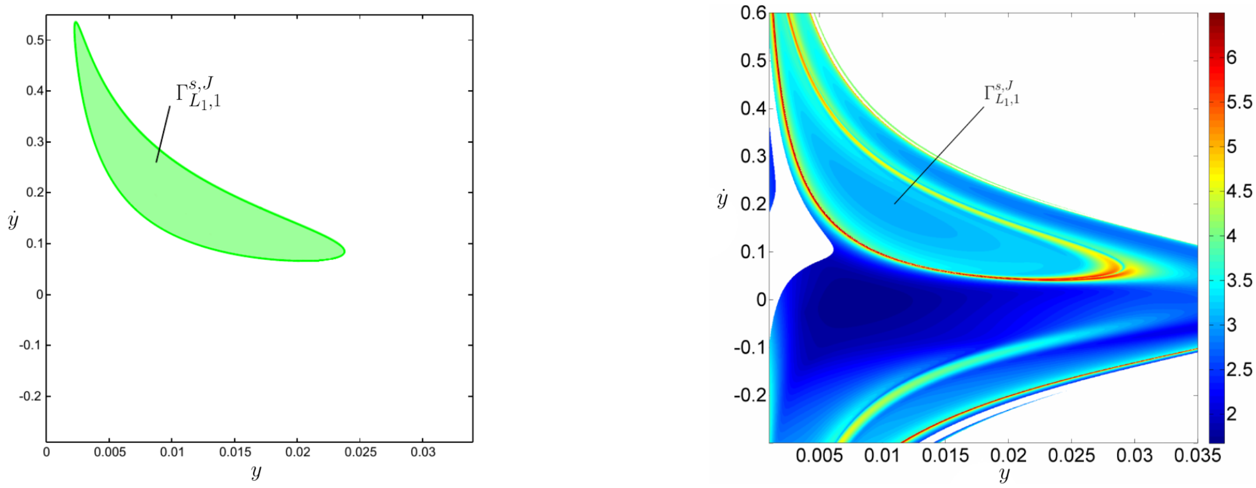

(a) Manifold intersection in the circular Sun-Jupiter system. (adapted from[1])

(b) FTLE field with $T = 1.5$ (positive time as dealing with stable manifolds) for the circular Sun-Jupiter system.

Figure 4. Comparison between the intersections on the $x = 1 - \mu$ plane of the stable manifold in the circular Sun-Jupiter system and the FTLE field on the same plane. Energy value fixed to $E = -1.519$.

B. Particles dynamics

Since LCS are separatrices of the motion,,[5,6] the phase space is still divided into regions with different dynamics (in the same fashion as manifolds). To verify this property the tool developed can be used. We set up a grid of particles (actually tracers of the dynamics) taken inside and outside a LCS of a generic Elliptic Restricted Three-body System ($\mu = 0.1, e = 0.04$). The FTLE map has been drawn on the $y = 0$ plane, fixing the energy to $E = -1.74$ and integrating for a time $T = 2.0$. The tracers initially placed inside the LCS in Fig. 5 are red colored, whereas the others are represented in blue.

The aim is to verify if the two set of tracers follow different dynamics as separated by the LCS computed; in particular it is expected, for manifold similarity, that the tracers placed inside the structures are the ones passing through the realm around the larger primary (where the section plane is placed) to the realm around the smaller primary (i.e. the transit behavior of the manifold structures in the CR3BP[1]). At the initial time, Fig. 6(a), the tracers are all crowded together and they cannot be distinguished. As time evolves, however, each tracer follows its own dynamics and the red tracers confirm to have a qualitatively different dynamics with respect to the blue tracers. In particular, after a sufficient time interval (2.0 TU in the case presented), all red tracers transited, as expected, in the realm around the smaller primary, leaving blue tracers orbiting around the larger primary, Fig. 6(d).

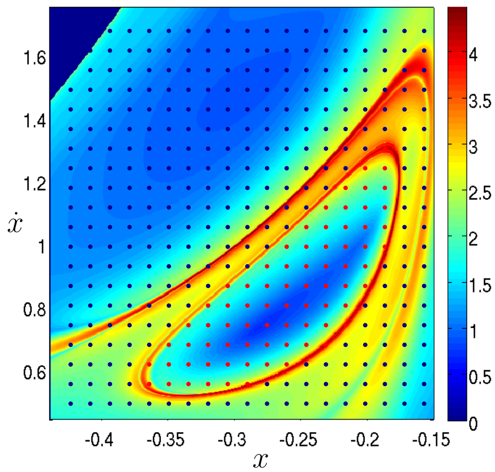

Figure 5. FTLE field at time $t_0 = 0$ on the $y = 0$ plane of an elliptic three-body system with $\mu = 0.1$ and $e = 0.04$. Integration time interval $T = 2$. Initial energy set to $E = -1.74$.

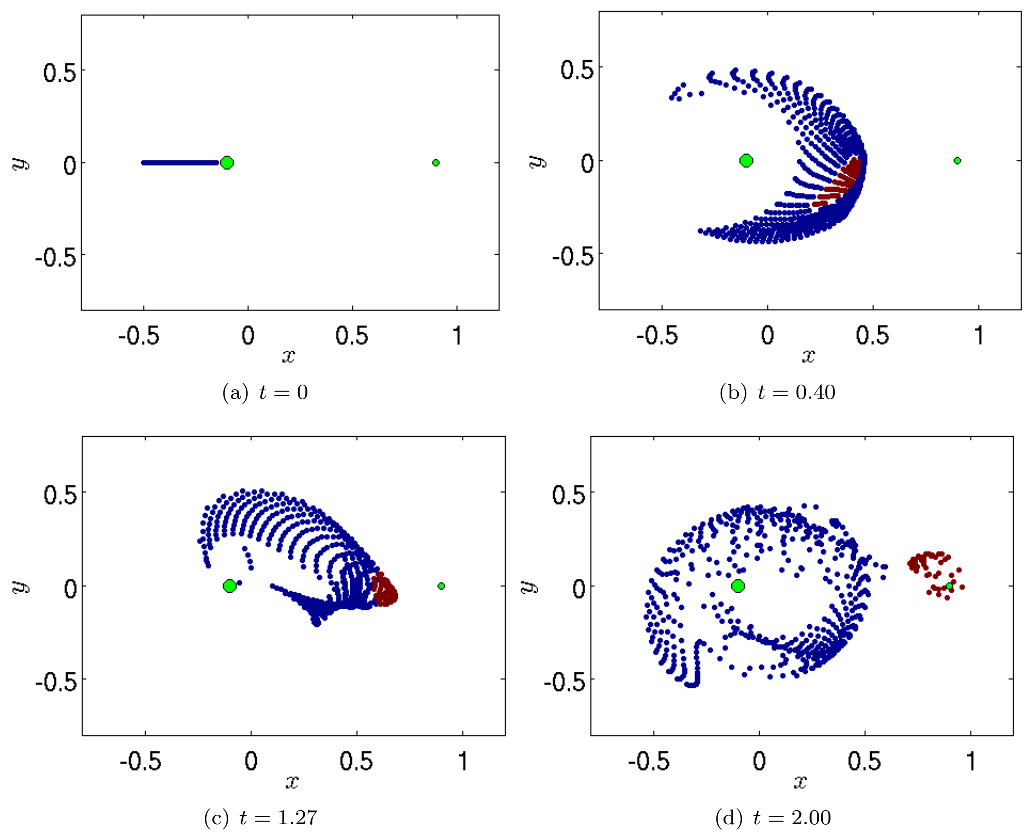

(a) $t = 0$

(b) $t = 0.40$

(c) $t = 1.27$

(d) $t = 2.00$

Figure 6. $\mu = 0.1$, $E = -1.74$, $e = 0.04$. Red tracers were taken inside the LCS of Fig. 5.

V. LCS Mission Design Methodology

We now present a practical design methodology for space missions based on LCS. In particular, we focus on interplanetary trajectories, although the same approach can be also used in planetary systems (e.g. the Earth-Moon system). Let us consider a transfer from Earth to one of the other planets of the Solar System. The specific Elliptic Three-body System is dependent on the choice of the target planet, which results in different values of the mass parameter μ and eccentricity e. The aim is to assess the complete mission starting from a parking Low Earth Orbit (LEO) and reaching a given final orbit around the destination planet. The interplanetary phase is designed by exploiting LCS computed in the Sun-planet Planar ER3BP system. Following a sort of patched conic approach, the whole transfer can be divided into three different phases according to the distance from the main attractor: the Earth escape and LCS injection phase, the interplanetary ballistic travel to the target planet and the injection in a closed target orbit. The three phases are divided by the two planets spheres of influence,[2] although this concept is not well defined in the ER3BP.

One fundamental hypothesis of the approach is to use a single impulse to perform the insertion maneuver into the LCS along with the Earth escape maneuver from a LEO orbit. This means that the velocity of the spacecraft at the Earth sphere of influence must match the velocity of a LCS point. This assumption implicitly considers that the LCS used for the transfer is located in the Earth vicinity; assumption confirmed by the behavior of the CR3BP manifold of the Sun-outer planet systems.[1] Figure 7(a) shows the geometry of the Earth escape maneuver.

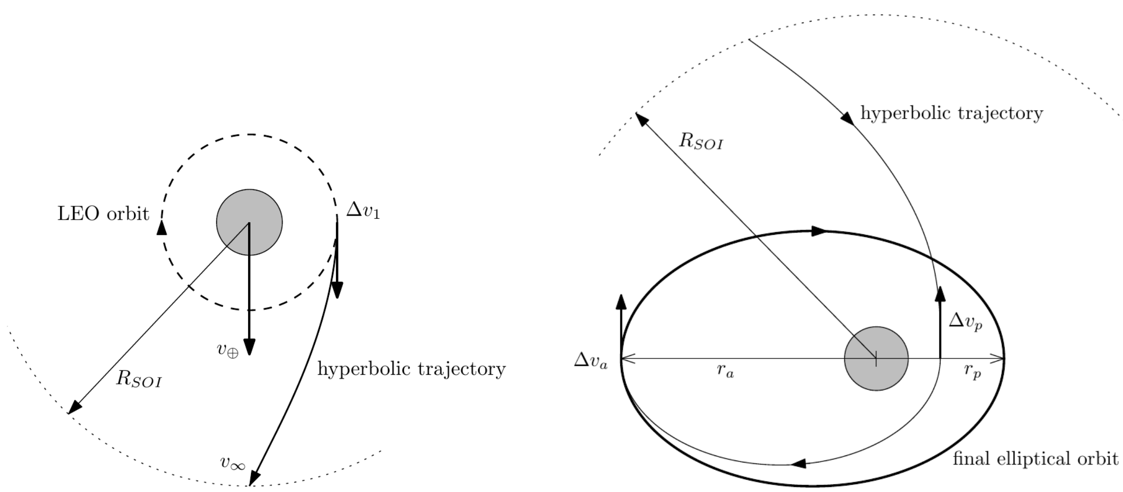

(a) **Geometry of the Earth escape maneuver.** (b) **Geometry of the final maneuver to close the orbit around the target planet.**

Figure 7. Impulsive maneuvers to escape from Earth sphere of influence and injection into the final orbit.

Considering a given departure date, ephemeris return Earth position and, therefore, the spacecraft x and y coordinates in the synodic reference frame (the Earth sphere of influence radius is neglected). The velocity components, needed to complete the spacecraft initial state vector, are varied in a proper range. This is done by means of a grid in the hodograph plane ($\dot{x} - \dot{y}$); physically this means to fire the thruster in all directions with variable intensity.

Now the equations of motion can be numerically integrated starting from each initial state and, by means of the procedure described in Sec. II.A, the FTLE field computed. Once the FTLE field has been obtained and visualized, its main structures can be identified. The specific dynamics they enclose can be understood by plotting a number of trajectories starting from different initial conditions close to these structures (as in the example of Sec. VI). To realize the transfer, the aim is to identify the set of initial conditions resulting in trajectories reaching the proximity of the target planet. Once such a set has been found, it is possible to define the arrival conditions at the target sphere of influence. The total Δv and transfer time required for the entire transfer for each point can be obtained. The total velocity change is given by the sum of the Δv needed for the LCS insertion and the Δv needed to close the orbit around the target planet. Among all these points the ones with the lower value of Δv or transfer time can be identified.

The initial maneuver is assumed to be a single burn from the Earth parking orbit to the LCS insertion.

The impulse injects the spacecraft in an escape hyperbola with a hyperbolic excess velocity matching the velocity needed for LCS injection. The corresponding Δv is evaluated by applying Keplerian spaceflight mechanics (assumed to be sufficiently accurate in the planet vicinity within the sphere of influence), although special attention must be paid to consider the proper reference frames. Values retrieved from the FTLE field are evaluated in the synodic Sun-planet frame, while the hyperbolic excess velocity is computed in a geocentric frame. Starting from the final velocity components, $\dot{x}$ and $\dot{y}$, the hyperbolic excess velocity can be found as:

$$v_\infty = \sqrt{(\dot{x} - \dot{x}_\oplus)^2 + (\dot{y} - \dot{y}_\oplus)^2} \tag{13}$$

where $\dot{x}_\oplus$ and $\dot{x}_\oplus$ are the components of Earth velocity in the synodic frame. Then, the semi-major axis of the escaping hyperbola a_h can be computed with:

$$a_h = -\frac{GM_\oplus}{v_\infty^2} \tag{14}$$

being $M_\oplus$ the mass of the Earth. The velocity at the perigee of the hyperbola, v_p, is:

$$v_p = \sqrt{GM_\oplus \left(\frac{2}{R_\oplus + h} - \frac{1}{a_h} \right)} \tag{15}$$

where h is the initial altitude of the LEO orbit and $R_\oplus$ the Earth radius.

Finally, Δv is computed as the difference between v_p and the circular velocity in the parking orbit

$$\Delta v = v_p - \sqrt{\frac{GM_\oplus}{R_\oplus + h}} \tag{16}$$

The final maneuver, aimed at closing the orbit around the target planet, starts at the target sphere of influence and it is assumed to be composed by two impulses. The first is implemented to set the apoapsis of the orbit at the target value, while the second sets the periapsis, as shown in Fig. 7(b).

The procedure for Δv computation is analogous to the previous one, taking into account the elliptic final orbit. Once in the Sphere Of Influence (SOI) of the target planet, the orbital parameters of the hyperbolic trajectory (a'_h, e'_h) can be inferred from the velocity at the end of the interplanetary trajectory (v_x, v_y). The arrival hyperbolic excess velocity is given by:

$$v_\infty = \sqrt{(v_x - v_{x_t})^2 + (v_y - v_{y_t})^2} \tag{17}$$

being (v_{x_t}, v_{y_t}) the orbital velocity of the target planet. From this, the semi-major axis a'_h and the eccentricity e'_h are given by:

$$a'_h = -\frac{GM_t}{v_\infty^2}, \qquad e'_h = \sqrt{1 - \frac{\boldsymbol{h} \cdot \boldsymbol{h}}{GM_t a'_h}} \tag{18}$$

where $\boldsymbol{h} = [0, 0, h_z] = \boldsymbol{r} \times \boldsymbol{v}$ is the angular momentum computed from the spacecraft position vector and velocity relative to the planet at its SOI, and M_t is the target planet mass.

A. Considerations

The exploitation of LCS for mission design purposes is not unique. The design approach itself depends on a number of variables and assumptions. Each of the assumptions we made in the approach outlined in Sec. V allows us to specify one or more of these variables. Nevertheless, some of them remain undetermined and have to be arbitrarily set, for instance based on specific mission requirements or the specific target planet. It is the case of the range over which the FTLE field is computed and visualized. In the hodograph plane this corresponds to set the allowed extreme values of the velocity components; constraint, for instance, given by the specific thruster available on-board. A broader range allows for exploring a wider span of the phase space and possibly to discover more different dynamical behaviors, but, at the same time, the resolution of the resulting picture could not be high enough to clearly distinguish structures in the FTLE field. Increasing the resolution implies a significantly higher computational time. On the other hand, a smaller range of velocity components shows a restricted part of the phase space, but allows a higher resolution and an easier identification of possible structures.

It might also happen that, even with a FTLE field computed at high resolutions (i.e. a large number of points along the two directions), no structure appears, or none of the structures exhibit the dynamical behavior sought. This could be due, most probably, to the integration interval chosen. If it is too short, trajectories do not have enough time to evolve in different dynamics and consequently the FTLE will have no evidence of these dynamics.

Dealing with the specific mission design approach proposed, several fundamental assumptions play a key role. The maneuvers type is fundamental for the computation of Δv; different thrust strategies would result in different Δv values. It is worth stressing, however, that this would also affect other fundamental steps of the procedure, such as the plane or the region over which compute the FTLE field. For example one could allow a different transfer strategy (e.g. a low-thrust spiraling out phase) transfer from the Earth to the injection into the LCS, thus also removing the constraint of the starting point coincident with the Earth position. The target orbit final maneuver could be changed as well as the time it is performed (in a low-thrust case, for instance, the deceleration maneuver might start well before the target sphere of influence).

With this approach the departure date has to be chosen before the analysis, so only the velocity vector can be varied. In Sec. VII it is shown a different method which allows for parametric study varying the date.

VI. Example of a Jupiter transfer

In this section we show the main results of the application of the design approach proposed to an interplanetary transfer to Jupiter. The Sun-Jupiter system has a mass parameter $\mu = 9.537 \times 10^{-4}$ and an eccentricity $e = 0.04839$. The considered departure date, arbitrarily set on the 9th July 2013, leads to the Earth position: $x_{\oplus} = -0.0245$, $y_{\oplus} = 0.1973$ in the non-dimensional synodic reference frame.

Figure 8 shows the FTLE field on the hodograph plane.

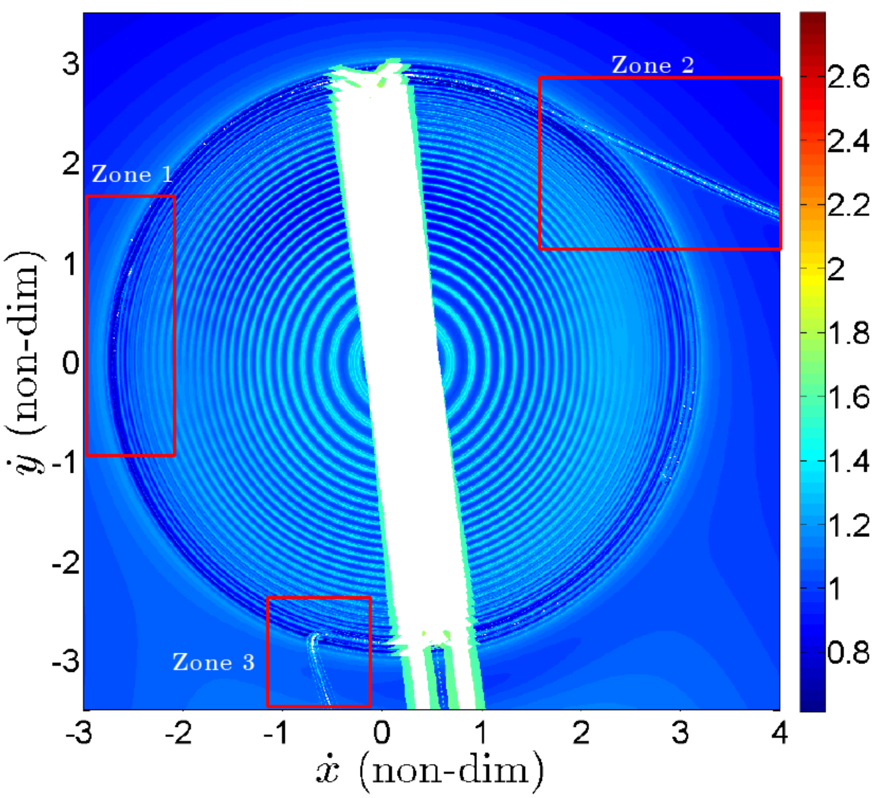

Figure 8. FTLE field at $t_0 =$ on the $\dot{x} - \dot{y}$ plane of the Sun-Jupiter elliptic system with position coordinates fixed at $x = -0.0245$, $y = 0.1973$.

The white stripe corresponds to orbits which result in a direct Sun collision (and thus have been discarded). Three different highlighted zones show some structures which have to be further investigate. Among them, the Zone 1 allows to maximize the effect of the Earth orbital velocity, as it is aligned with the final velocity to achieve. To proceed with the transfer design, however, we need a more detailed picture of the FTLE field in that zone. Figure 9(a) shows a refinement of the FTLE field in the region of interest.

The region around the LCS has been sampled by means of a grid of initial conditions (see Fig. 9(b)), which has been integrated forward in time until reaching the Jupiter sphere of influence, where the final orbit injection takes place. We considered a Galileo-like final orbit with an apojove radius $r_a = 1751500$ km and a perijove radius $r_p = 285900$ km.[15] We computed the Δv for each point of the grid as shown in Fig. 10(a).

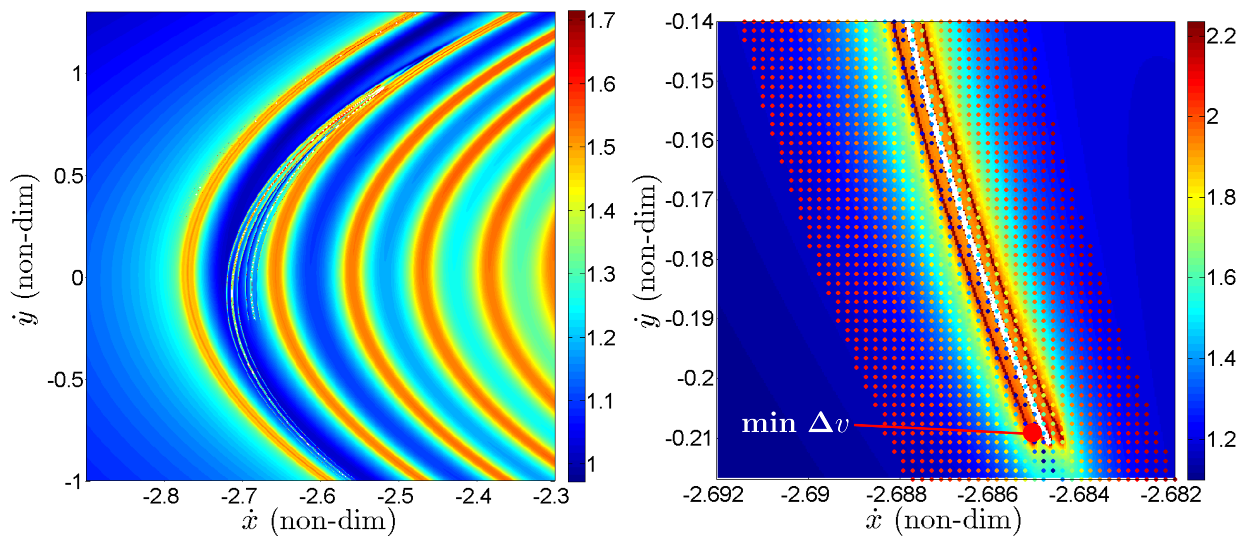

(a) **Zone 1 of Fig. 8.**

(b) **Grid of initial conditions (dots) on a detail of Zone 1**

Figure 9. Further investigation of Zone 1

On this graph, the best point in terms of Δv results to be the one with $\dot{x} = -2.6849$ and $\dot{y} = -0.2123$, with an associated $\Delta v = 7.10$ km/s and a transfer time of 9 years and 3 months. The trajectory relative to the best point in therms of Δv is shown in Fig. 10(b).

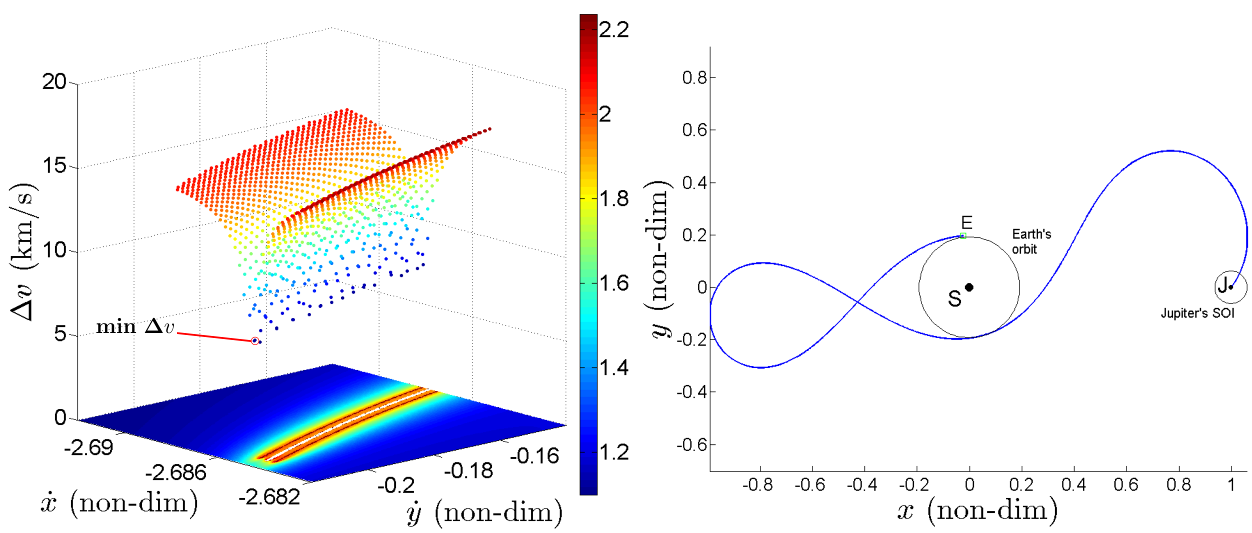

(a) Distribution of initial points in terms of Δv

(b) Best trajectory in terms of Δv in the Sun-Jupiter synodic frame.

Figure 10. Best point in terms of Δv is $\dot{x} = -2.6849$ and $\dot{y} = -0.2123$, with an associated $\Delta v = 7.10$ km/s and a transfer time of 9 years and 3 months.

VII. Parametric studies

A possible modification of the approach proposed in Sec. V is to constrain the direction of the departure velocity at the insertion into the LCS, while allowing a parametric study on the starting date. In this modified procedure, the departure direction is assumed to be tangent to the Earth orbit, thus taking the maximum advantage from the Earth orbital velocity for the interplanetary ballistic transfer inside the LCS. In this way only the velocity magnitude V is the free parameter. In addition it might be useful not to restrict to a specific departure date, but varying the starting position along the whole Earth orbit. To account for both of these needs a new independent variable, the Earth anomaly ν (measured from the Jupiter perihelion), is introduced. For each couple of parameters $\nu - V$ an initial point can be identified and from this it is possible to retrieve the $x, y, \dot{x}, \dot{y}$ coordinates required for the FTLE computation. To do so it is necessary to arbitrarily define the initial condition perturbations to compute the $\nabla\phi$ matrix, see Eq. (11). In particular we have chosen dx=d$y = 0.001$, d$\dot{x}$=d$\dot{y} = 0.001$ in non-dimensional units. These parameters are not required for the procedure outlined in Sec. V, as the step of the grid itself defines the initial state perturbation. Once the FTLE values are computed, the resulting FTLE field is plotted directly on the $\nu - V$ plane, Fig. 11 shows the complete grid over one Jupiter period.

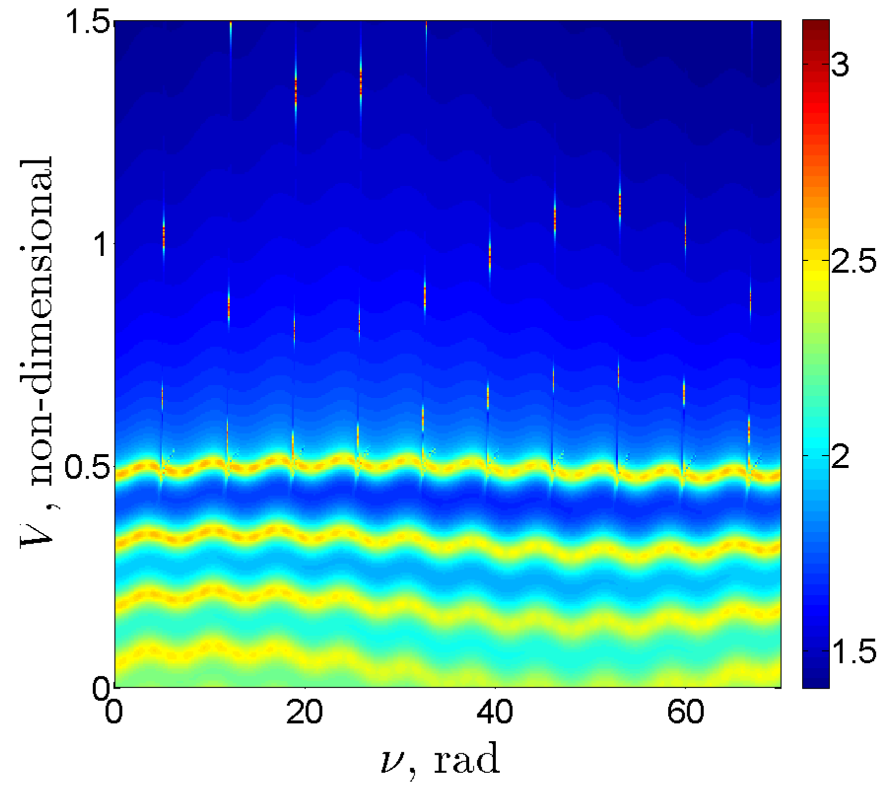

Figure 11. FTLE field on the $\nu - V$ plane over a entire Jupiter period.

To refine the analysis, as an example we explored the interval $\nu \in [14.5, 16.5]$ rad, which corresponds to about three months around the 9th of July 2013, as shown in Fig. 12. Also in this case it is possible to identify some structures that can be further analyzed by means of trajectories plotting, as shown in Fig. 12(b).

With this approach it is possible to get rid of a specific departure date and many unfeasible departure conditions (like the ones in the withe strip in Fig. 8) are not integrated at all with a significant saving in the computation time. Moreover a parametric study of the most convenient launch configuration can be done and the whole set of possible transfer dynamics identified at once.

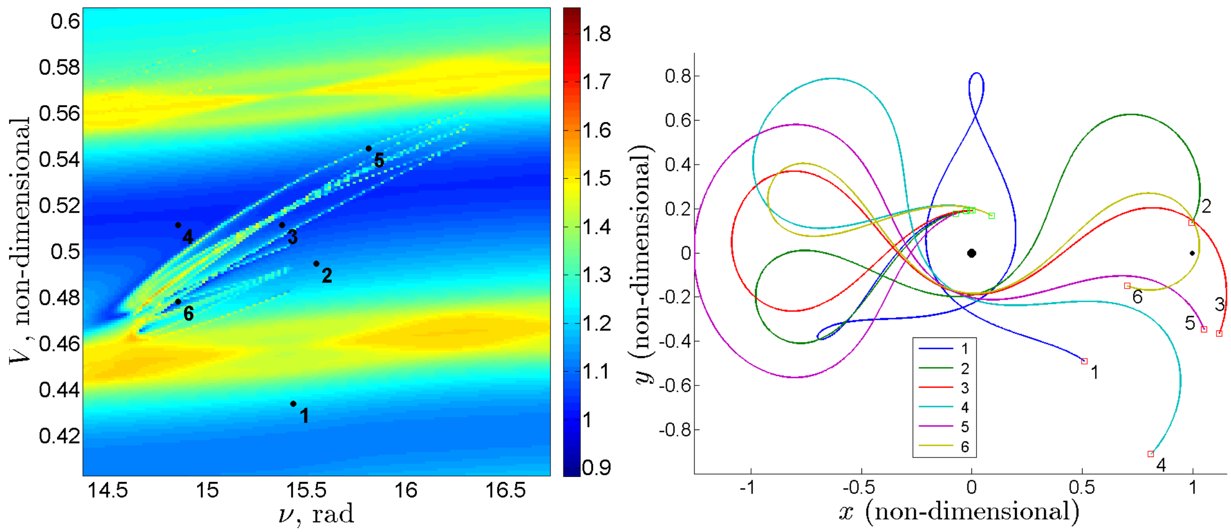

(a) **Starting points**

(b) **Trajectories**

Figure 12. Several trajectories integrated for $T = 5$ in the Sun-Jupiter system. Initial points chosen in an interval of 55 days, with an initial velocity relative to the Earth as shown on the vertical axis.

VIII. Conclusion

The application of Lagrangian Coherent Structures allows for a manifold-like analysis of the elliptic restricted three-body problem. Thus, this kind of system can be used since the early mission design phases. The approach proposed for designing a space mission in such a way starts from the Earth sphere of influence and maps all possible interplanetary trajectories identifying those close to LCS. Once the best LCS candidate has been identified, a grid of initial condition has been used to implement the mission approach considered (single burn escape and two burns capture). Furthermore, the generalization of the procedure proposed based on the Earth anomaly and on a tangential escape velocity, allows for a parametric study of all possible Earth-target planet relative configurations. In this way several transfer dynamics can be identified (all using different LCS), so that the additional mission constraints (e.g. transfer time, Sun or other planets distances) can be satisfied. The approach we proposed resulted in a preliminary design of a transfer from Earth to Jupiter exploiting the natural dynamics of the Planar Elliptic Sun-Jupiter System. As shown in Sec. VII, it is possible to modify the approach to fit the mission constraints and assumptions.

The possible exploitations of LCS in elliptic systems for preliminary mission design are likely unlimited. One possible approach can be seeking for persistent or time varying intersections among structures in different systems. In this way it is possible to think of a time dependent series of natural interplanetary connections throughout the Solar System, extending the concept of the Interplanetary Transport network, as it has already been pointed out for the CR3BP.[16] The wide margins for development, however, are given by the potentiality of Lagrangian Coherent Structures as a tool for exploring behavior of dynamical systems. The Planar Elliptic Restricted Three-body Problem is only one possible system to be analyzed. The first extension one can think of is the ER3BP in its spatial formulation. But the possibilities are not confined to Three-body systems. For example, a four body formulation can be used to better analyze the Earth-Moon system considering the perturbation of the Sun. Furthermore, one could include other perturbations in the R3BP not excluding the presence of a low thrust propulsion device.

References

[1]Koon W.S., Lo M.W., Marsden J.E. and Ross S.D., *Dynamical Systems, the Three-Body Problem and Space Mission Design*, Marsden Books, 2011.

[2]Pergola P., Geurts K., Casaregola C., Andrenucci M., *Three-Body Invariant Manifold Transition with Electric Propulsion*, Springer Space Technology Library - Space Manifold Design, 2009.

[3]Peacock T. and Dabiri J., “Introduction to Focus Issue: Lagrangian Coherent Structures”, *Chaos*, 2010.

[4]Ritcher J. P., *The literary work of Leonardo Da Vinci*, 1970.

[5]Haller G., "Finding finite-time invariant manifolds in two-dimensional velocity fields", *Chaos*, Vol. 10, 2000.

[6]Haller G. and Yuan G., "Lagrangian coherent structures and mixing in two-dimensional turbulence", *Physica D*, Vol. 147, pp. 352-370, 2000.

[7]Mathur M. and Haller G. Peacock T., Ruppert-Felsot J. E., Swinney H. L., "Uncovering the Lagrangian Skeleton of Turbulence", *Physical Review Letters*, Vol. 98, April 2007.

[8]Gawlik E., Marsden J., Du Toit P., Campagnola S., "Lagrangian Coherent Structures in the Elliptic Restricted Three-Body Problem", *Celestial Mechanics and Dynamical Astronomy*, Vol. 103 No. 3, pp. 227-249, 2009

[9]Szebehely V. and Giacaglia G., "On the Elliptic Restricted Problem of Three Bodies", *Astronomical Journal*, Vol. 69, No. 3, April 1964.

[10]Szebehely V., *Theory of Orbits in the Restricted Problem of Three Bodies*, Academic Press, New York, 1967.

[11]Pérez D., Gomez G. and Masdemont J., "Detecting invariant manifolds using hyperbolic Lagrangian Coherent Structures", *Proceedings of the 1st IAA Conference on Dynamics and control of Space Systems*, 2012.

[12]Shadden S., Lekien F., Marsden J., "Definition and properties of Lagrangian coherent structures from finite-time Lyapunov exponents in two-dimensional aperiodic flows", *Physica D*, Vol. 212, pp. 271-304, 2005.

[13]Eberly D., Gardner R., Morse B. and Pizer S., "Ridge for image analysis", *Journal of Mathematical Imaging and Vision*, Vol. 4, pp. 355-371, 1994.

[14]Ahnert K. and Mulansky M., "Odeint - Solving ordinary differential equations in C++", *AIP Conference Proceedings*, Vol. 1389, pp. 1586-1589, 2011.

[15]Galileo mission profile, URL: http://starbrite.jpl.nasa.gov/pds/viewMissionProfile.jsp?MISSION_NAME=galileo, [cited 30 June 2013].

[16]Ross S., "The Interplanetary Transport Network", *American Scientist*, Vol. 94, No. 3, pp. 230-237, 2006.